

PHYSICOCHEMICAL ANALYSIS
OF INORGANIC SYSTEMS

Tl₂S–Sb₂S₃–Bi₂S₃ Quasi-Ternary System

Ya. I. Dzhafarov and M. B. Babanly

Baku State University, Baku, Azerbaijan

Received May 5, 2008

Abstract—The Tl₂S–Sb₂S₃–Bi₂S₃ quasi-ternary system (system A) was studied using DTA, X-ray powder diffraction, microstructure examination, and microhardness measurements. TlSbS₂–Tl₄Bi₂S₅ (TlBiS₂, Bi₂S₃), Sb₂S₃–TlBiS₂, Tl₃SbS₃–TlBiS₂(Bi₂S₃), and [TlSb_{0.5}Bi_{0.5}S₂]–Tl₂S isopleths; isothermal sections at 500 K; and liquidus surface projection of system A were constructed. Characteristic features of the title system are extensive fields of solid solutions extended along the TlSbS₂–TlBiS₂ quasi-binary section and a continuous solubility belt 1–2 mol % wide extended along the Sb₂S₃–Bi₂S₃ binary subsystem. Primary separation fields of phases and the types and coordinates of invariant and monovariant equilibria in system A were determined.

DOI: 10.1134/S0036023609110254

Search for new multicomponent phases and development of electronic materials on their base require studying phase equilibria in the relevant systems. In this context, quasi-ternary planes of such systems containing binary and ternary allied compounds are of most interest on account of possible formation of extensive solid solutions.

This work continues our studies [1–3] concerning the search for and creation of physicochemical fundamentals for the preparation of four-component phases of variable composition based on thallium, antimony, and bismuth chalcogenides. Here, our efforts were focused on phase equilibria in the Tl₂S–Sb₂S₃–Bi₂S₃ system (system A).

Physicochemical parameters of the starting compounds of system A are found in [4, 5]. The compounds Tl₂S, Sb₂S₃, and Bi₂S₃ melt congruently at 723, 819, and 1050 K, respectively. The Tl₂S structure is rhombohedral (CdI₂ antitype): $a = 12.22 \text{ \AA}$, $c = 18.21 \text{ \AA}$, space group $\bar{R}\bar{3} - C_{3i}^2$. Sb₂S₃ and Bi₂S₃ crystallize in orthorhombic system (space group $Pbmn - D_{2h}^{16}$) with the parameters $a = 11.20 \text{ \AA}$, $b = 11.28 \text{ \AA}$, $c = 3.83 \text{ \AA}$ and $a = 11.13 \text{ \AA}$, $b = 11.27 \text{ \AA}$, $c = 3.97 \text{ \AA}$, respectively.

The Tl₂S–Sb₂S₃, Tl₂S–Bi₂S₃, and Sb₂S₃–Bi₂S₃ boundary subsystems of system A were studied earlier [4, 6–8].

The Tl₂S–Sb₂S₃ [6, 7] and Tl₂S–Bi₂S₃ [8] quasi-binary systems form several compounds, some melting congruently (Tl₃SbS₃ (610 K), TlSbS₂ (755 K), and TlBiS₂ (1040 K)) and the others incongruently (TlSb₃S₅ (683 K), TlSb₅S₈ (693 K), and Tl₄Bi₂S₅ (820 K)).

Sb₂S₃–Bi₂S₃ [4] is also a quasi-binary section; its phase diagram shows the complete solubility of the

components in liquid and solid states without extremes on the liquidus and solidus curves.

Thallium thiostibnites and thiobismuthites have the following structures and crystal parameters: Tl₃SbS₃ (rhombohedral space group $R\bar{3}m$, $a = 9.552 \text{ \AA}$, $c = 7.306 \text{ \AA}$) [9], TlSbS₂ (rhombohedral space group $R\bar{3}m$, $a = 9.519 \text{ \AA}$, $c = 7.364 \text{ \AA}$) [10], TlSb₃S₅ (monoclinic space group $P2_{1/c}$, $a = 7.225 \text{ \AA}$, $b = 15.547 \text{ \AA}$, $c = 8.946 \text{ \AA}$, $\alpha = 113.54^\circ$), TlSb₅S₈ (monoclinic space group Pn , $a = 8.098 \text{ \AA}$, $b = 19.415 \text{ \AA}$, $c = 9.059 \text{ \AA}$, $\alpha = 91.96^\circ$) [9], TlBiS₂ (hexagonal space group $\bar{R}\bar{3}m$, $a = 4.12 \text{ \AA}$, $b = 21.9 \text{ \AA}$) [11], Tl₄Bi₂S₅ (orthorhombic space group $Pnma6_2$, $a = 16.760 \text{ \AA}$, $b = 4.09 \text{ \AA}$, $c = 17.396 \text{ \AA}$, $Z = 4$) [12].

Earlier [13], Dzhafarov studied phase equilibria in system A within the TlSbS₂–TlBiS₂–Bi₂S₃–Sb₂S₃ region. TlSbS₂–TlBiS₂ (Bi₂S₃) and Sb₂S₃–TlBiS₂ isopleths and a 500-K isotherm of the phase diagram were constructed, as well as the liquidus surface projection for this subsystem. The TlSbS₂–TlBiS₂ isopleth was shown to be quasi-binary and eutectic with incomplete terminal solid solutions. The eutectic contains 86 mol % TlSbS₂ and melts at 740 K. The homogeneity regions of the terminal solid solutions based on TlSbS₂ (γ_1) and TlBiS₂ (γ_2) at the eutectic temperature have maximal extents of 0–10 and 68–100 mol % TlBiS₂, respectively. The homogeneity regions narrow with decreasing temperature, at 500 K being 0–7 and 72–100 mol % TlBiS₂, respectively.

EXPERIMENTAL

For use in the phase diagram design for the Tl₂S–Sb₂S₃–Bi₂S₃ system (system A), binary com-

Table 1. Invariant equilibria in the $\text{Ti}_2\text{S}-\text{Sb}_2\text{S}_3-\text{Bi}_2\text{S}_3$

Point in Fig. 3	Equilibrium	Composition, mol %		<i>T</i> , K
		Ti_2S	Sb_2S_3	
D_1	$\text{L} \longleftrightarrow \text{Ti}_3\text{SbS}_3$	75	25	610
D_2	$\text{L} \longleftrightarrow \text{TiSbS}_2$	50	50	755
D_3	$\text{L} \longleftrightarrow \text{TiBiS}_2$	50	—	1040
e_1	$\text{L} \longleftrightarrow \text{Ti}_2\text{S} + \text{C}_3$	80	20	596
e_2	$\text{L} \longleftrightarrow \gamma_1 + \text{C}_3$	71	29	592
e_3	$\text{L} \longleftrightarrow \gamma_1 + \text{C}_1$	28	72	665
e_4	$\text{L} \longleftrightarrow \text{Ti}_2\text{S} + \text{C}_4$	94	—	713
e_5	$\text{L} \longleftrightarrow \gamma_2 + \beta$	25	—	948
e_6	$\text{L} \longleftrightarrow \gamma_1 + \gamma_2$	50	44	740
e_7	$\text{L} \longleftrightarrow \gamma_2 + \text{C}_3$	73	24	600
p_1	$\text{L} + \text{C}_2 \longleftrightarrow \text{C}_1$	27	73	683
p_2	$\text{L} + \beta \longleftrightarrow \text{C}_2$	24	76	693
p_3	$\text{L} + \gamma_2 \longleftrightarrow \text{C}_4$	82	—	815
E_1	$\text{L} \longleftrightarrow \gamma_1 + \beta + \text{C}_1$	27	67	650
E_2	$\text{L} \longleftrightarrow \gamma_1 + \gamma_2 + \text{C}_3$	70	28	585
E_3	$\text{L} \longleftrightarrow \text{Ti}_2\text{S} + \text{C}_3 + \text{C}_4$	80	19	590
P_1	$\text{L} + \text{C}_2 \longleftrightarrow \text{C}_1 + \beta$	25	71	675
P_2	$\text{L} + \gamma_2 \longleftrightarrow \gamma_1 + \beta$	28	60	695
P_3	$\text{L} + \gamma_2 \longleftrightarrow \text{C}_3 + \text{C}_4$	75	22	595

Note: Phase notations: $\text{C}_1 = \text{TiSb}_3\text{S}_5$, $\text{C}_2 = \text{TiSb}_5\text{S}_8$, $\text{C}_3 = \text{Ti}_3\text{SbS}_3$, $\text{C}_4 = \text{Ti}_4\text{Bi}_2\text{S}_5$, $\gamma_1 = \text{TiSbS}_2$ -base solid solution, $\gamma_2 = \text{TiBiS}_2$ -base solid solution, and β = terminal solid solutions extending along the $\text{Sb}_2\text{S}_3-\text{Bi}_2\text{S}_3$ binary subsystem.

compounds Ti_2S , Sb_2S_3 , and Bi_2S_3 and ternary compounds Ti_3SbS_3 , TiSbS_2 , TiSb_3S_5 , TiSb_5S_8 , $\text{Ti}_4\text{Bi}_2\text{S}_5$, and TiBiS_2 were synthesized by alloying their constituent elements in vacuo ($\sim 10^{-2}$ Pa) and identified.

Alloys of system **A** along various sections ($\text{TiSbS}_2-\text{Ti}_4\text{Bi}_2\text{S}_5$, $\text{Ti}_3\text{SbS}_3-\text{Ti}_4\text{Bi}_2\text{S}_5$ (TiBiS_2 , Bi_2S_3), and $[\text{TiSb}_{0.5}\text{Bi}_{0.5}\text{S}_2]-\text{Ti}_2\text{S}$) and beyond these sections

were prepared by alloying the constituent compounds in evacuated quartz glass ampoules. Onset melting temperatures were determined from the thermoanalytical curves of cast unhomogenized alloys. Homogenizing anneals lasting ~ 800 h were carried out slightly (20–30 K) below the onset melting temperatures. Then, all alloys were additionally annealed at 500 K for ~ 400 h.

The investigative tools were DTA (NTR-73 pyrometer, Chromel/Alumel thermocouples), X-ray powder diffraction (DRON-3, CuK_α radiation), microstructure examination (MIM-7), and microhardness measurements (PMT-3 microhardness tester).

RESULTS AND DISCUSSION

Analyzing our experimental results and literature data on the quasi-binary boundary subsystems and the $\text{TiSbS}_2-\text{TiBiS}_2$ inner section, we gained the global pattern of phase equilibria in system **A**.

Below, you will find $\text{Ti}_3\text{SbS}_3-\text{TiBiS}_2(\text{Bi}_2\text{S}_3)$, $\text{TiSbS}_2-\text{Ti}_4\text{Bi}_2\text{S}_5$, and $[\text{TiSb}_{0.5}\text{Bi}_{0.5}\text{S}_2]-\text{Ti}_2\text{S}$ isopleths (Figs. 1a–1d), an 500-K isothermal section (Fig. 2), and the liquidus-surface projection (Fig. 3) for system **A**.

The types and coordinates of all invariant and monovariant equilibria of system **A** are displayed in Tables 1 and 2.

The data at hand imply that the $\text{Ti}_2\text{S}-\text{Sb}_2\text{S}_3-\text{Bi}_2\text{S}_3$ system is a quasi-ternary plane of the $\text{Ti}-\text{Sb}-\text{Bi}-\text{S}$ quaternary system.

$\text{TiSbS}_2-\text{TiBiS}_2$ is the only quasi-binary isopleth of system **A** [13].

The $\text{Ti}_3\text{SbS}_3-\text{TiBiS}_2$ isopleth (Fig. 1a) in the solid state crosses $\text{C}_3 + \text{C}_4 + \gamma_2$ and $\text{C}_4 + \gamma_2$ heterogeneous fields ($\text{C}_3 = \text{Ti}_3\text{SbS}_3$ and $\text{C}_4 = \text{Ti}_4\text{Bi}_2\text{S}_5$). The liquidus consists of two branches that refer to the primary separations of C_3 and γ_2 phases. As a result of eutectic and peritectic monovariant reactions (Table 2; curves e_7P_3 , p_3P_3), below liquidus the system enters $\text{L} + \text{C}_3 + \gamma_2$ and $\text{L} + \text{C}_4 + \gamma_2$ three-phase states. The horizontal of the invariant peritectic reaction (Table 1, P_3) extends from 100 to 28 mol % Ti_3SbS_3 . Within 28–2 mol % Ti_3SbS_3 , final solidification follows the monovariant peritectic reaction p_3P_3 (Table 2).

The $\text{Ti}_3\text{SbS}_3-\text{Bi}_2\text{S}_3$ isopleth (Fig. 1b) in the solid state crosses two-phase fields ($\gamma_1 + \gamma_2$, $\beta + \gamma_2$) and three-phase fields ($\text{C}_3 + \gamma_1 + \gamma_2$ and $\beta + \gamma_1 + \gamma_2$). The liquidus consists of three branches that refer to the primary separations of C_3 , γ_2 , and β phases. Below-liquidus curves refer to $\text{L} \leftrightarrow \text{C}_3 + \gamma_2$, $\text{L} \leftrightarrow \gamma_1 + \gamma_2$, and $\text{L} \leftrightarrow \beta + \gamma_2$ monovariant eutectic reactions (Table 2). As a result, $\text{L} + \text{C}_3 + \gamma_2$, $\text{L} + \gamma_1 + \gamma_2$, and $\text{L} + \beta + \gamma_2$ three-phase fields appear. Within 2–45, 49–51, 45–49, and 51–100 mol % Ti_3SbS_3 , final solidification follows e_5P_2 and e_6E_2 (e_6P_2)

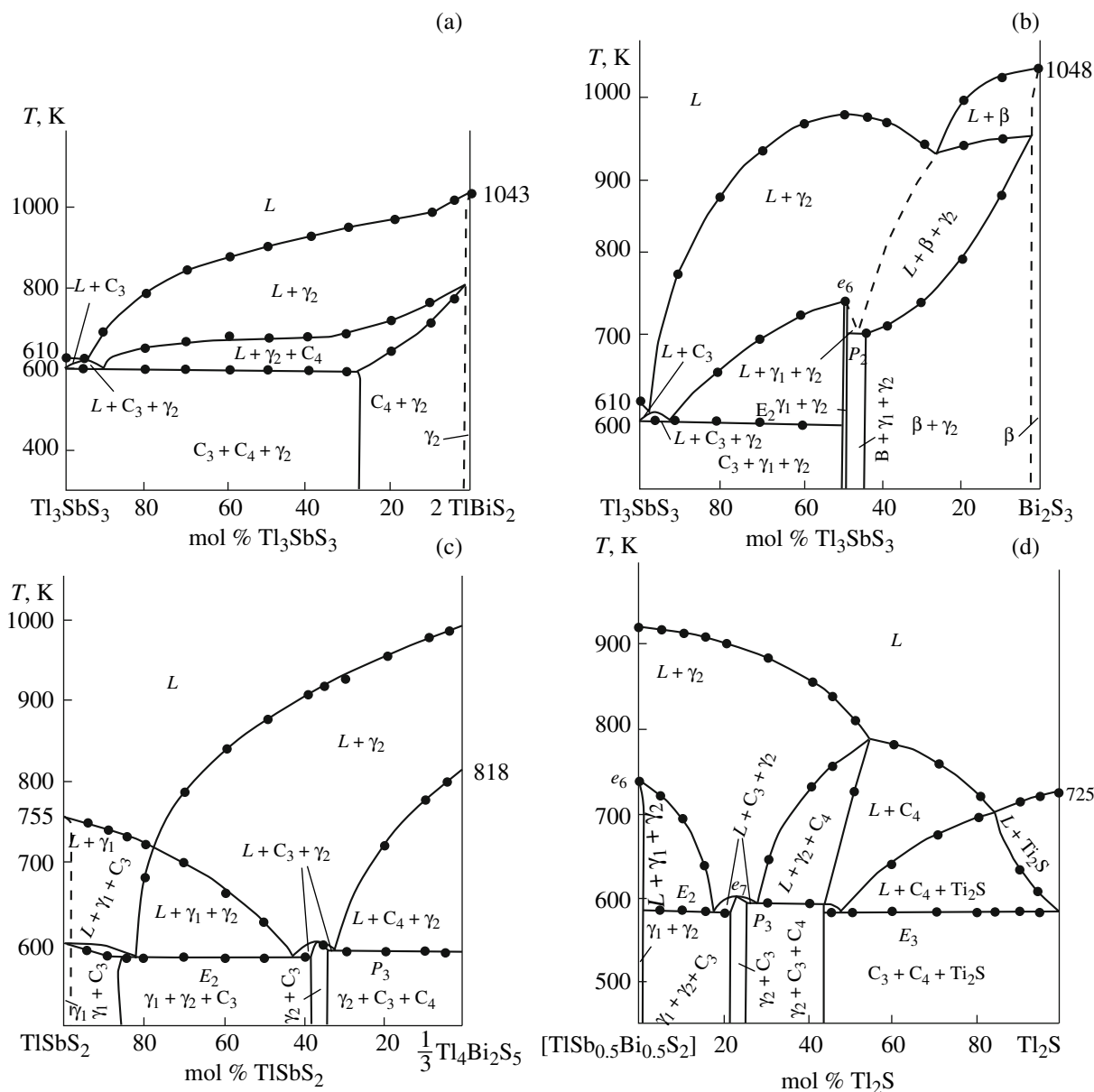


Fig. 1. Phase diagrams of (a) TL₃SbS₃–TlBiS₂ (b) TL₃SbS₃–Bi₂S₃, (c) TlSbS₂–Tl₄Bi₂S₅, and (d) [TlSb_{0.5}Bi_{0.5}S₂]–Tl₂S sections of the TL₂S–Sb₂S₃–Bi₂S₃ system.

monovariant reactions and P_2 and E_2 invariant reactions (Tables 1, 2).

We also studied TlSbS₂(Tl₃SbS₃)–Tl₄Bi₂S₅ and [TlSb_{0.5}Bi_{0.5}S₂]–Tl₂S isopleths of system A with their numerous heterogeneous equilibria (Figs. 1c, 1d). The [TlSb_{0.5}Bi_{0.5}S₂]–Tl₂S isopleth is useful to disclose the sequence of equilibrium phase transformations both in liquid–solid state and in the subsolidus region of the TL₂S–TlSbS₂–TlBiS₂ subsystem. The joint consideration of Figs. 1c, 1d, 2, and 3 is helpful to determine heterogeneous equilibria, which are reflected on the TlSbS₂–Tl₄Bi₂S₅ and [TlSb_{0.5}Bi_{0.5}S₂]–Tl₂S isopleths.

Figure 2 displays our version of the global pattern of solid-phase equilibria in system A at 500 K. The β , γ_1 , and γ_2 solid solution fields lie as bands 1–2 mol % wide along the Sb₂S₃–Bi₂S₃ and TlSbS₂–TlBiS₂ systems. The two- and three-phase fields are dominated by solid solutions based on congruently melting compounds. More exact positions of phase-field boundaries were determined using microstructure analysis and microhardness measurements. Alloys containing 0–7 and 72–100 mol % TlBiS₂ in the TlSbS₂–TlBiS₂ system at 500 K are single phases. Microhardness in these alloys ranges from ~900 to ~1100 MPa and from ~850 to ~700 MPa, respectively.

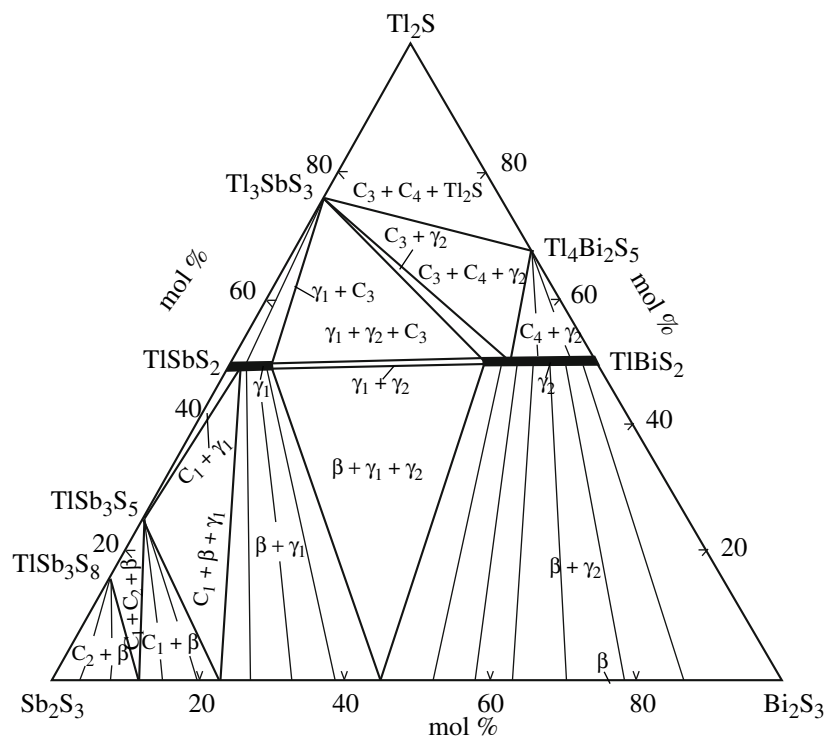


Fig. 2. 500-K isothermal section of the Tl_2S – Sb_2S_3 – Bi_2S_3 phase diagram.

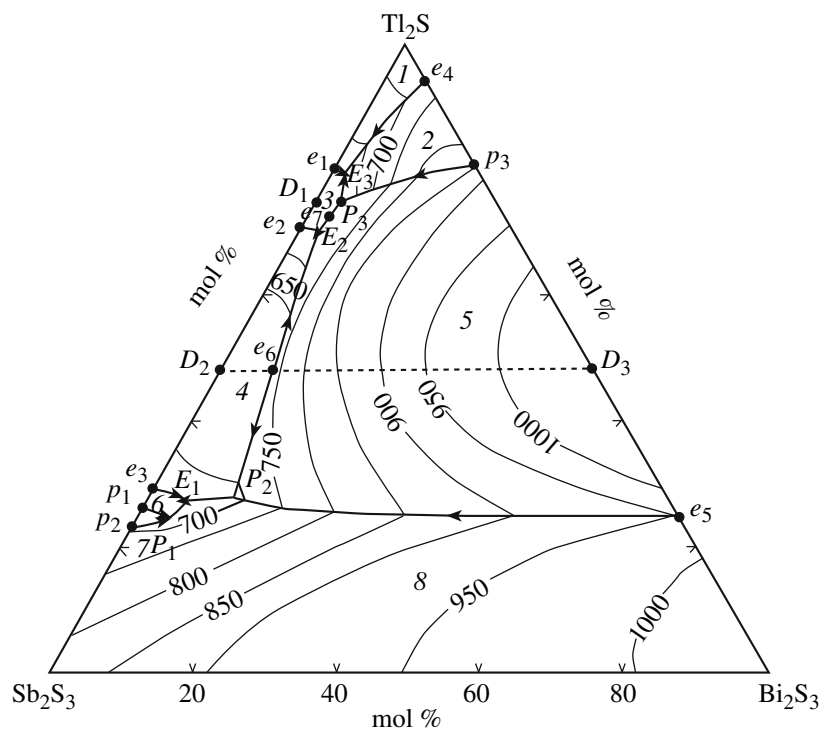


Fig. 3. Liquidus surface projection for the Tl_2S – Sb_2S_3 – Bi_2S_3 system. Primary crystallization fields: (1) Tl_2S , (2) C_4 , (3) C_3 , (4) γ_1 , (5) γ_2 , (6) C_1 , (7) C_2 , and (8) β .

Table 2. Monovariant equilibria in the TL₂S–Sb₂S₃–Bi₂S₃

Curve in Fig. 3	Equilibrium	Temperature range, K
e_1E_3	$L \longleftrightarrow \text{TL}_2\text{S} + C_3$	596–590
e_2E_2	$L \longleftrightarrow \gamma_1 + C_3$	592–585
e_3E_1	$L \longleftrightarrow \gamma_1 + C_1$	665–650
e_4E_3	$L \longleftrightarrow \text{TL}_2\text{S} + C_4$	713–590
e_6E_2	$L \longleftrightarrow \gamma_1 + \gamma_2$	740–585
e_7E_2	$L \longleftrightarrow \gamma_2 + C_3$	600–585
e_5P_2	$L \longleftrightarrow \gamma_2 + \beta$	948–695
e_6P_2	$L \longleftrightarrow \gamma_1 + \gamma_2$	740–695
e_7P_3	$L \longleftrightarrow \gamma_2 + C_3$	600–595
p_1P_1	$L + C_2 \longleftrightarrow C_1$	683–675
p_2P_1	$L + \beta \longleftrightarrow C_2$	693–675
p_3P_3	$L + \gamma_2 \longleftrightarrow C_4$	815–595
P_1E_1	$L \longleftrightarrow \beta + C_1$	675–650
P_2E_1	$L \longleftrightarrow \gamma_1 + \beta$	695–650
P_3E_3	$L \longleftrightarrow C_3 + C_4$	595–590

The liquidus surface of system A (Fig. 3) consists of eight primary crystallization fields. The β - and γ_2 phases have most extensive fields, which allows melt compositions for single crystal growth to be varied.

An interesting feature of system A is that saddle point e_7 does not lie on a quasi-binary join.

REFERENCES

- M. B. Babanly, S. M. Veisova, Z. A. Guseinov, and Ya. I. Dzhafarov, *Zh. Neorg. Khim.* **47** (6), 1020 (2002) [Russ. J. Inorg. Chem. **47** (6), 917 (2002)].
- Ya. I. Dzhafarov, A. M. Mirzoeva, and M. B. Babanly, *Zh. Neorg. Khim.* **51** (5), 871 (2006) [Russ. J. Inorg. Chem. **51** (5), 805 (2006)].
- Ya. I. Dzhafarov, A. M. Mirzoeva, and M. B. Babanly, *Zh. Neorg. Khim.* **53** (1), 153 (2008) [Russ. J. Inorg. Chem. **53** (1), 146 (2008)].
- N. Kh. Abrikosov, *Chalcogenide Semiconductors and Their Alloys* (Nauka, Moscow, 1975) [in Russian].
- The Physicochemical Properties of Semiconductor Materials. A Handbook*, Ed. by A. V. Novoselova and V. B. Lazarev (Nauka, Moscow, 1979) [in Russian].
- J.-C. Jumas, E. Olivier-Fourcade, N. Rey, and E. Philipot, *Rev. Chim. Miner.* **22** (5), 651 (1985).
- M. B. Babanly, Yu. A. Yusibov, and V. T. Abishov, *Electromotive Force in the Thermodynamics of Compound Semiconductors* (Izd-vo BGU, Baku, 1992) [in Russian].
- M. B. Babanly, M. F. Kesamanly, and A. A. Kuliev, *Zh. Neorg. Khim.* **33** (5), 2371 (1988).
- Yu. V. Voroshilov, T. L. Evstigneeva, and I. Ya. Nekrasov, *The Crystal-Chemical Tables for Ternary Chalcogenides* (Nauka, Moscow, 1989) [in Russian].
- F. W. Dikson and A. S. Radtke, *Am. Mineral.* **63** (7, 8), (1978).
- M. Julien-Pouzel and M. Guittard, *Bull. Soc. Chim. Fr.*, Nos. 5–6, 1037 (1975).
- M. Julien-Pouzel, S. Saulmas, and P. Laruelle, *Acta Crystallogr., Sect. B*: **35** (6), 1313 (1979).
- Ya. I. Dzhafarov, *Nauch. Tr. Az. Tekhn. Univ., Ser. Fundam. Nauk*, No. 1, 57 (2008).